In Vitro/In Vivo Comparison of Drug Release and Polymer Erosion from Biodegradable P(FAD-SA) Polyanhydrides—A Noninvasive Approach by the Combined Use of Electron Paramagnetic Resonance Spectroscopy and Nuclear Magnetic Resonance Imaging

Karsten Mäder,[1,5] Yannick Crémmilleux,[2] Abraham J. Domb,[3] Jeffrey F. Dunn,[4] and Harold M. Swartz[4]

Received December 9, 1996; accepted March 6, 1997

Purpose. The purpose of this study was to compare drug release and polymer erosion from biodegradable P(FAD-SA) polyanhydrides *in vitro* and *in vivo* in real time and with minimal disturbance of the investigated system.

Methods. P(FAD-SA) 20:80 and P(FAD-SA) 50:50 polymer tablets were loaded with the spin probe 3-carboxy-2,2,5,5-tetramethyl-pyrrollidine-1-oxyl (PCA) and implanted subcutaneously in the neck of rats or placed in 0.1 M phosphate buffer. 1.1 GHz EPR spectroscopy experiments and 7T MRI studies (T1 and T2 weighted) were performed.

Results. A front of water penetration was visible by MRI *in vitro* in the case of P(FAD-SA) 20:80, but not for P(FAD-SA) 50:50. For both polymers, the thickness of the tablets decreased with time and a insoluble, easy deformable residue remained. Important processes such as edema, deformation of the implant, encapsulation and bioresorption were observable by MRI *in vivo.* P(FAD-SA) 50:50 was almost entirely absorbed by day 44, whereas an encapsulated residue was found for P(FAD-SA) 20:80 after 65 days. The EPR studies gave direct evidence of a water penetration induced changes of the microenvironment inside the tablet. EPR signals were still detectable in P(FAD-SA) 20:80 implants after 65 days, while the nitroxide was released *in vitro* within 16 days.

Conclusions. Important parameters and processes such as edema, deformation of the tablet, microviscosity inside the tablet and encapsulation can be monitored in real time by the combined use of the noninvasive techniques MRI and EPR leading to better understanding of the differences between the *in vitro* and *in vivo* situation.

KEY WORDS: biodegradable polymers; EPR; MRI; drug delivery; *in vitro/in vivo* correlation.

INTRODUCTION

Although biodegradable polymers are now used clinically for the treatment of various diseases (1,2), there is only limited knowledge about the processes involved in the degradation and erosion of implants *in vivo,* as well as the *in vivo* mechanisms of drug release. A critical point in the design of delivery devices is understanding the mechanisms of polymer degradation and drug delivery and whether there are any differences between these processes *in vivo* and *in vitro.* To answer this question, appropriate techniques are needed which can monitor the key processes and key parameters of drug release and polymer erosion *in vivo* in real time, without disturbing the sample. Unfortunately, the most frequently applied analytical methods such as chromatography, microscopy, calorimetry or infrared spectroscopy require surgical extraction an do not meet these criteria. Radioactive labeled molecules as model drugs provide only information concerning the concentration of the labeled compound and require a special synthesis.

The noninvasive method of Magnetic Resonance Imaging (MRI) is widely used clinically as a diagnostic tool. MRI monitors the local concentration and the physical state of protons. Therefore, MRI can potentially be used to characterize the penetration of water into the polymer implant, which is a key event in the release of the drug and degradation of the polymer. It has been shown *in vitro* that MRI can be applied to follow the hydration process of tablets and to characterize the state of water in terms of proton relaxation times or self diffusion coefficients (3,4). MRI has been also been used *in vivo* to detect the presence of a biodegradable implant in the monkey brain (5) and to follow the release of gadolinium compounds from implants (6,7). Recently it has been demonstrated that MRI may also be used to characterize the biodegradable drug delivery system itself *in vivo* (8).

EPR spectroscopy is a noninvasive analytical technique which can provide unique information in pharmacy (9). Recently, low frequency EPR spectrometers have been developed which make studies *in vivo* feasible (10,11). The sensitivity of the equipment is sufficient to detect drug derived free radicals directly *in vivo* and to study the impact of antioxidants on their formation (12). Unique information can be obtained by EPR in the field of drug delivery (13,14) using nitroxide radicals as model drugs. The EPR spectra are sensitive to the nitroxide mobility as illustrated in Fig. 1. In addition to the measurement of nitroxide mobility, pH measurements inside the delivery systems are possible using specially designed nitroxides. A polymer degradation induced pH drop from 4 to 2 inside subcutaneously implanted PLGA-tablets has been reported recently (15).

It has been demonstrated that MRI and EPR can give complementary information regarding the processes of polymer erosion and drug release (8). However, the MRI and EPR experi-

[1] Institute of Pharmacy Humboldt-University Berlin, Goethestr. 54, 13086 Berlin, Germany.

[2] Laboratoire de RMN, CPE, Universite Claude Bernard Villeurbanne Cedex, France.

[3] School of Pharmacy, The Hebrew University Jerusalem, 91120 Jerusalem, Israel.

[4] Dept. of Radiology, Dartmouth Medical School Hanover, New Hampshire 03755, USA.

[5] To whom correspondence should be addressed. (e-mail: Karsten=Maeder@rz.hu-berlin.de)

ABBREVIATIONS: EPR, electron paramagnetic resonance spectroscopy; FAD, fatty acid dimer (dimer of erucic acid = 13,14 dioctyl-octacosane-1,28-dioic acid); MRI, magnetic resonance imaging; PCA, 3-carboxy-2,2,5,5-tetramethylpyrrollidine-1-oxyl; P(CPP-SA), poly(1,3-bis-p-carboxyphenoxypropane-co-sebacic anhydride); P(FAD-SA), poly(fatty acid dimer—sebacic acid anhydride); PSA, poly(sebacic acid anhydride); SA, sebacic acid, (= decanedioic acid); T1W, T1 weighted; T2W, T2 weighted.

0724-8741/97/0600-0820$12.50/0

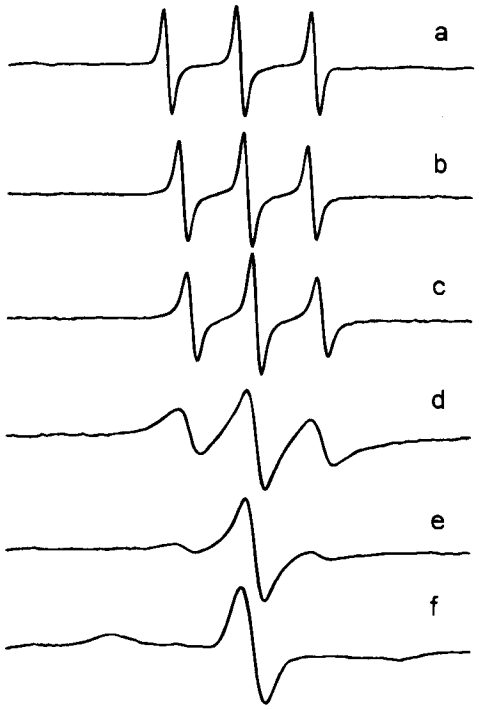

Fig. 1. Influence of the mobility of the PCA environment on the spectral shape of 1.1 GHz EPR spectra: a: water 20 °C; b: molten hard fat, 70 °C; c: hard fat at melting point, 33 °C; d: hard fat at 20 °C; e: hard fat at 5 °C, f: immobilized in dry methocell 20 °C (solid powder).

ments were performed on different animals. The aim of the present work is to evaluate the mechanisms of drug release and polymer erosion from P(FAD-SA) polyanhydrides by the combined use of the noninvasive techniques EPR and MRI *in vitro* and *in vivo* (using the same animals). In order to quantify the MRI signal intensity of the tablet core we decided to use muscle tissue as an internal standard. Due to the fact that paramagnetic nitroxide radicals may act as contrast agents (16) we also compared the MR images of P(FAD-SA) tablets with and without PCA.

MATERIALS AND METHODS

Chemicals

The spin probe PCA (3-Carboxy-2,2,5,5-tetramethylpyrrollidine-1-oxyl) was purchased from Aldrich Chemicals. Poly(-fatty acid dimer—sebacic acid) (P(FAD-SA)) polymers were synthesized as previously described (17). The fatty acid dimer (FAD) 13,14-dioctyl-octacosane-1,28-dioic acid is a dimer derivative of erucic acid. Hard fat (Witepsol® H15) was obtained from Hüls GmbH, Germany) and Methocell from FLUKA AG, Switzerland).

Sample Preparation

PCA-loaded tablets (3 mmol/kg polymer) tablets of 8.6 mm in diameter and 2 mm thickness were prepared by melt molding (90°C, 2 min) in a home made teflon device. The tablets were allowed to cool down slowly for 30 minutes at room temperature. Thereafter, the samples were stored under nitrogen atmosphere for 5 days at −15°C.

In Vitro Studies

The tablets were placed in 20 ml 0.1 M phosphate buffer, pH 7.4 at 37°C. The buffer was changed daily. The polymer samples were removed and handled without mechanical damage. For EPR measurements, the tablet were rinsed carefully with fresh buffer solution to remove nitroxide molecules from the surface. The water film at the surface was removed by blotting carefully with an absorbent paper. The tablets were put in airtight plastic boxes during the measurements to avoid drying. In the case of the *in vitro* MRI evaluation of P(FAD-SA) 50:50 it was necessary to put the tablets in a hydrogel (Aerosil in water 10% m/m), because otherwise no image contrast was obtained by the tablet itself. All studies were carried out in triplicate.

In Vivo Studies

The *in vivo* studies were performed according to an approved protocol and adhered to the principles of laboratory animal care (NIH publication #85-23, revised 1985). PCA loaded tablets were implanted subcutaneously into the neck (dorsal side) of anesthetized (Ketamine/Xylazine 100/20 mg/kg) male Wistar rats (200–300 g). EPR and MRI measurements were performed on the same anesthetized animals. Each group had three animals.

EPR-Spectroscopy

EPR spectra were recorded using a home built 1.1 GHz spectrometer equipped with a surface coil using the following parameters: central magnetic field B_0 = 42 mT, scan range = 10 mT, incident microwave power = 40 mW, amplitude of modulation = 0.1 mT, scan time = 300 s, time constant = 0.3 sec.

Magnetic Resonance Imaging

MR imaging was performed with a 7.0 T horizontal bore Magnex magnet and a SMIS system. The rats were anesthetized and placed supine over a home designed "butterfly" shaped RF surface coil. Axial spin-echo T1 and T2 weighted sequences (T1: repetition time = 500 ms, echo time = 16 ms; T2: repetition time = 1800 ms, echo time = 50 ms) were used. Other imaging parameters were 4 acquisitions, number of slices = 7, slice thickness = 2mm, field of view = 40 mm, and image matrix = 128 × 128. The signal intensity of muscle tissue was used as an internal standard to quantify the signal intensity of the tablet core.

RESULTS

Magnetic Resonance Imaging

In Vitro

No MRI image was attainable with dry tablets. MRI Signal enhancement from outside to inside as well as a decrease of the tablet thickness was observed for P(FAD-SA) 20:80 after exposure to 0.1M phosphate buffer (Fig. 2, top). In contrast, exposure to buffer did not result in MRI contrast enhancement for P(FAD-SA) 50:50 tablets. To be able to obtain MRI images under these circumstances we placed the P(FAD-SA) tablets in

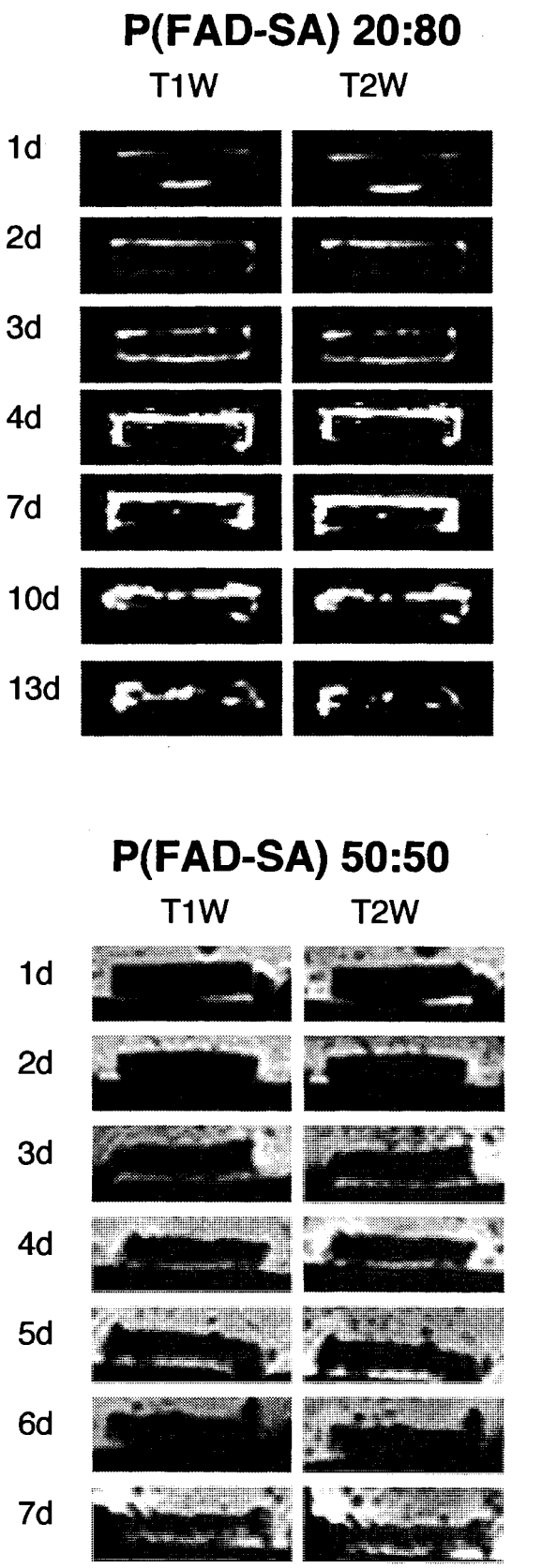

Fig. 2. *In vitro* MR T1 and T2 weighted images of PCA loaded 2 mm thick tablets consisting of P(FAD-SA) 20:80 (left) and P(FAD-SA) 50:50 (right) after different times of exposure to 0.1 M phosphate buffer, pH 7.4.

a 10% (m/m) Aerosil hydrogel. The images clearly show also a decrease of the tablet thickness with time. (Fig. 2, bottom). No differences in the MRI signal intensity were observed between nitroxide loaded and unloaded samples for P(FAD-SA) 20:80 and 50:50.

In Vivo

A decrease of the tablet thickness within the first week was observable for subcutaneously implanted P(FAD-SA) 20:80 tablets (Fig. 3). A layer of degraded polymer on the tablet surface is clearly visible at day 3. Bright areas around the tablet are detected between day 5 and 10. These bright areas are likely to be local interstitial fluid. The P(FAD-SA) 20:80 implants lost their shape after 2 weeks and encapsulation by tissue (seen as similar contrast on T1W and T2W images) became visible. There is little difference between the images from day 16 to day 65. The images showed a dark, deformed tablet core, surrounded by degraded polymer which was encapsulated. The MRI signal intensity inside the tablet core did increase with time, but did not exceed the intensity of muscle tissue (Fig. 4).

The P(FAD-SA) 50:50 implants also showed a decrease of the tablet thickness during the first days (Fig. 5). Deformed implants, surrounded by degraded polymer and water are visible on the images on day 8 and 10. The water around the implant disappears in the following days and encapsulation of the implant is visible. In contrast to P(FAD-SA) 20:80 there is a considerable decrease in the size of the encapsulated area and only traces of the implant remained after 44 days. A modest increase in signal intensity of the tablet core was observed (Fig. 6).

Electron Paramagnetic Resonance Spectroscopy

In Vitro

The nitroxide is released from the polyanhydrides within 14 days (P(FAD-SA) 20:80) or 7 days (P(FAD-SA) 50:50). The kinetics of release correspond closely to first order kinetics (Fig. 7). The EPR spectra of dry P(FAD-SA) tablets showed a higher mobility of the spin probe compared to polyanhydrides composed of poly-sebacic-acid (PSA) or poly(1,3-bis-p-carboxyphenoxypropane-co-sebacic anhydride) 20:80 (P(CPP-SA) 20:80) (8), indicating that the nitroxide is molecular solubilized in the polymer. In addition to the observed decrease of the EPR signal intensity, changes of the spectral shape were detected (Fig. 8; left side), showing a water penetration induced modification of the microenvironment inside the tablet. Surprisingly, the distance between the maximum of the first and the minimum of the last peak (indicated by the arrows) increased with time, which indicates a decrease of the nitroxide mobility. The decreased nitroxide mobility was also reflected by the increase of the ratio of the signal amplitudes between the second and the third peak. In addition, a spectral contribution of water solubilized, rapid tumbling nitroxide molecules was detectable after day 3 (marked by the asterix in Fig. 8). Similar, although less pronounced spectral changes were also detectable for P(FAD-SA) 50:50 polymers.

In Vivo

In addition to a decrease in signal intensity, changes of the spectral shape were also detectable for subcutaneously

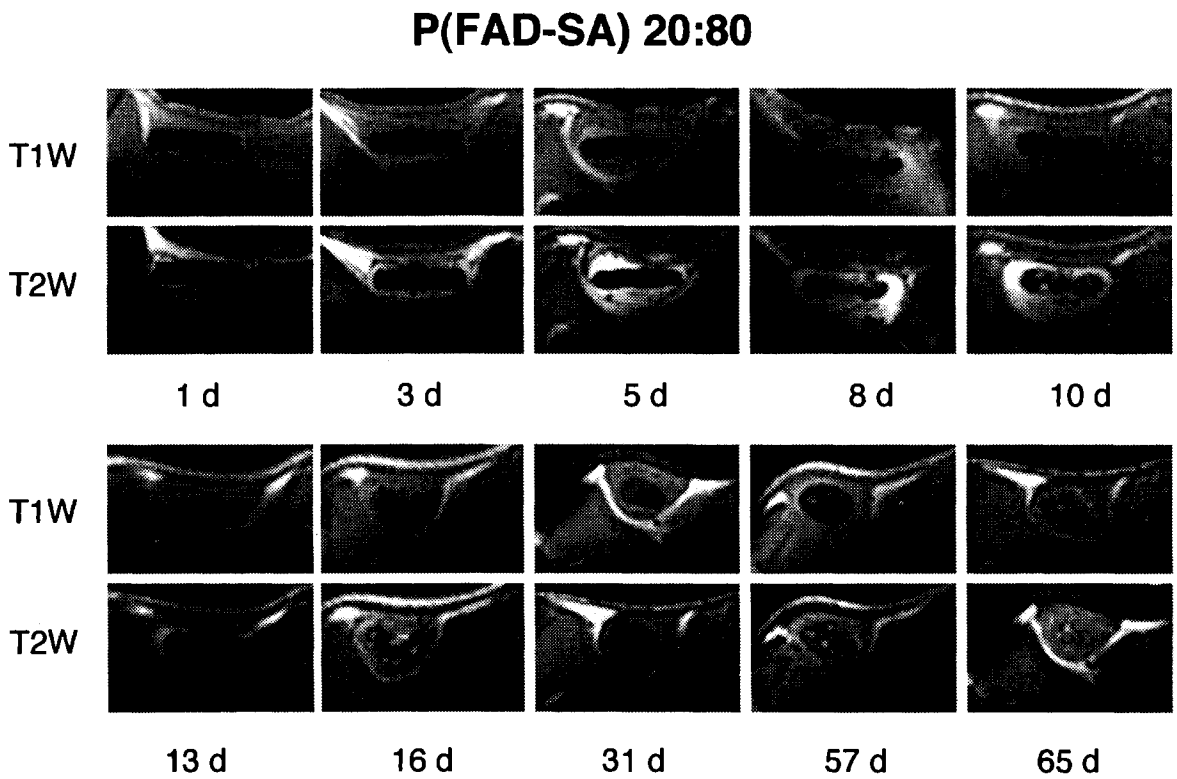

Fig. 3. *In vivo* MR T1 and T2 weighted images of PCA loaded 2 mm thick subcutaneously implanted P(FAD-SA) 20:80 tablets.

implanted P(FAD-SA) 20:80 tablets (Fig. 8; right side). The spectral shape of the EPR spectra recorded in vivo 10 days after implantation of the polymer is typical for water solubilized, highly mobile nitroxide molecules (see also Fig. 1a). There was almost no change in the spectral shape and the signal intensity between day 16 and 65.

The decrease in nitroxide mobility during the first days was also observed for P(FAD-SA) 50:50 implants. The release was completed within 2 weeks, which is slower compared to *in vitro* release of the same polymer, but faster compared to the *in vivo* release from P(FAD-SA) 20:80 implants.

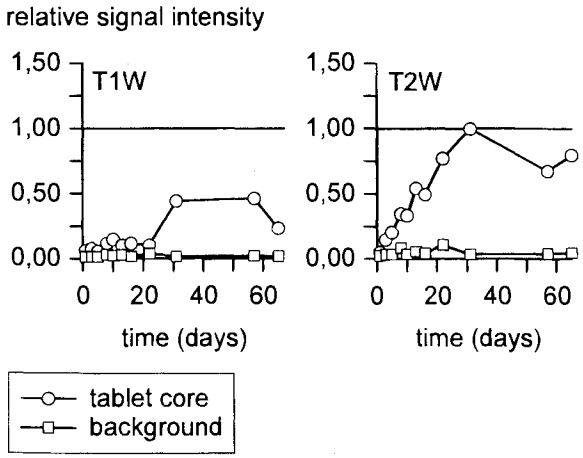

Fig. 4. Time dependency of the relative signal intensity (1 = muscle) of the P(FAD-SA) 20:80 implant core in T1 (left) and T2 (right) weighted MRI images.

DISCUSSION

The experimental results demonstrate the ability of magnetic resonance techniques to characterize processes of drug delivery and polymer erosion noninvasively *in vitro* and *in vivo*. ^{1}H-MRI signal intensity depends mainly on two factors, the total amount of ^{1}H nuclei and appropriate relaxation times. No MRI signal enhancement was visible in dry tablets, although the polymers are mainly composed of protons. This is not surprising because the transverse relaxation times can be very short in solid matrices. Water penetration into P(FAD-SA) 20:80 tablets induced signal enhancement from outside to inside, but no enhancement was seen for P(FAD-SA) 50:50 tablets. This result is consistent with previous studies with light microscopy, which indicated that the erosion zone differs between the two polymers (18). A porous, white solid and fragile zone was described for P(FAD-SA) 20:80 whereas a clear, viscous zone was observed for P(FAD-SA) 50:50. It was also found that the content of free water does not exceed 5 wt % for P(FAD-SA) 20:80 and 3 wt % for P(FAD-SA) 50:50 (19). We conclude that the higher *in vitro* MRI signal intensity of P(FAD-SA) 20:80 is due to the increased porosity and higher water content of the erosion zone.

Early MRI visible changes indicate eroded polymer material around an intact implant core for both polymers *in vivo*. Later, the implants lost their shape. This process may contribute to different release rates by altering the surface area of the delivery system. The earlier deformation time of P(FAD-SA) 50:50 (at day 8) compared to P(FAD-SA) 20:80 (day 16) corresponds to a lower melting point (62–66°C vs. 72–77°C) (17) and lower crystallinity (37% vs. 53%) (19) of this polymer. The signal enhancement of the tablets increased with time (Figs.

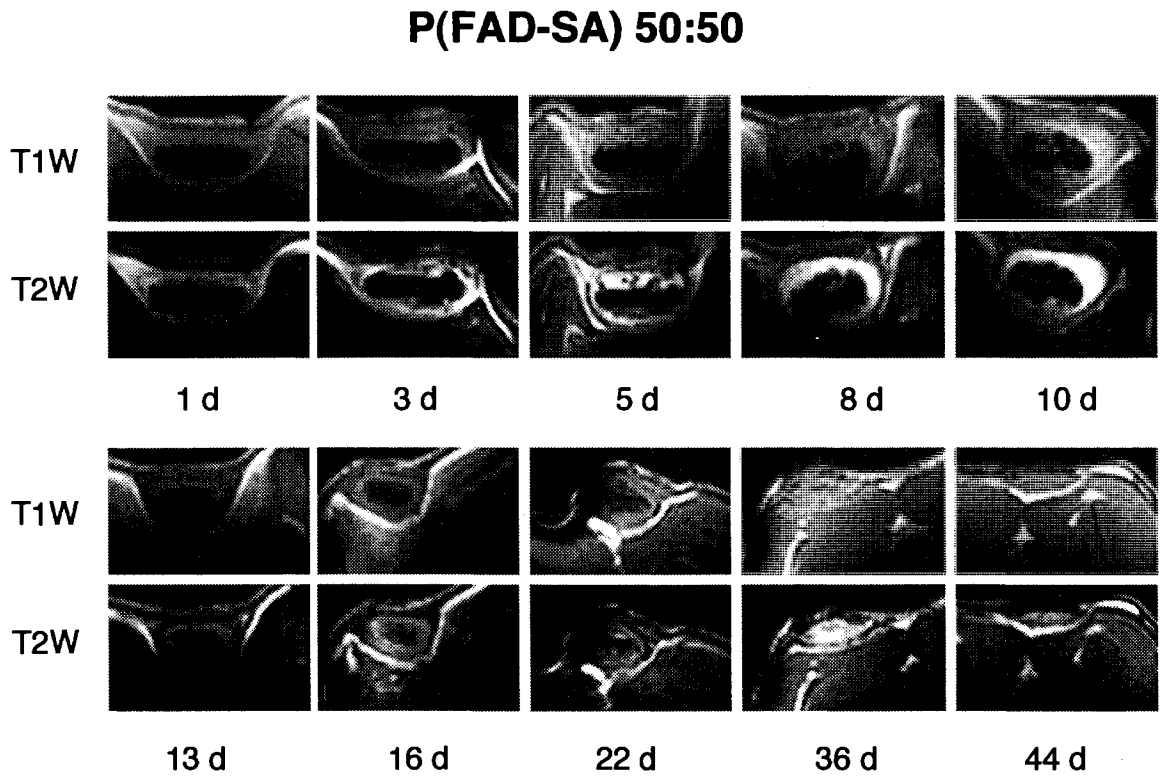

Fig. 5. *In vivo* MR T1 and T2 weighted images of PCA loaded 2 mm thick subcutaneously implanted P(FAD-SA) 20:80 tablets.

4 and 6). The increase in signal intensity, however, was 4 to 10 times lower compared to P(CPP-SA) 20:80 or PSA respectively (8). This is because the eroded zones differ between these polymers. Also, as reported previously, polymer erosion from P(CPP-SA) 20:80 and PSA did not change the overall thickness of the polymer tablets for a long time (8, 20) while a decrease of the thickness was observed for the P(FAD-SA) polymers in the present study and related experiments (18). The differences in the characteristics of polymer erosion are due to the fact that the incorporation of FAD is associated with a higher flexibility and lower crystallinity of the polymer matrix.

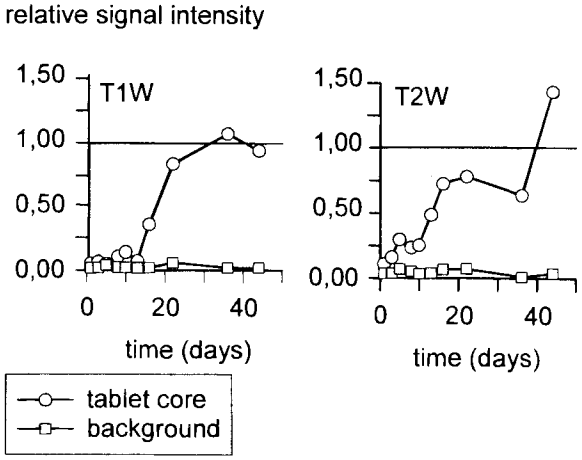

Fig. 6. Time dependency of the relative signal intensity (1 = muscle) of the P(FAD-SA) 50:50 implant core in T1 (left) and T2 (right) weighted MRI images.

An important finding of this study was the fact, that both polymers are encapsulated *in vivo*. Encapsulation is associated with a decreased polymer clearance. A dark tablet core was still visible for P(FAD-SA) 20:80 after 65 days. In contrast, only traces were found of the less crystalline 50:50 polymer after 44 days. We assume that different crystallinity of the polymers may be an important factor for this observation. However, the polymer erosion rate seems also to be important, because no encapsulation was observed for the more hydrophilic PSA, which has a higher crystallinity, but degrades much more rapidly compared to P(FAD-SA) 20:80 (8).

The faster release of PCA observed *in vitro* may be due to a higher availability of water. Also, a higher buffer capacity has to be taken into account, because polymer erosion from polyanhydrides has been shown to be pH-dependent (21). Although to a different extent, the water penetration induced changes of the shape of the EPR spectra were qualitatively the same for both polymers: (1) initially an increase in the distance between the maximum of the first and the minimum of the third peak accompanied with an increase of the ratio of the signal amplitudes of the second to the third peak and (2) later, the appearance of a spectral contribution from a water solubilized nitroxide. Observation (1) indicates a decreased mobility of the nitroxide in the polymer matrix. It has been shown, that water penetrates into P(FAD-SA) polymers of comparable thickness within 24 hours and a increased mobility inside the polymer might be expected (19). However, this water is almost completely consumed for the hydrolysis of the anhydride bonds, leading to the formation of the monomers SA and FAD. Because formation of monomers by polyanhydride hydrolysis is much faster than release of the monomers, crystallization of poorly

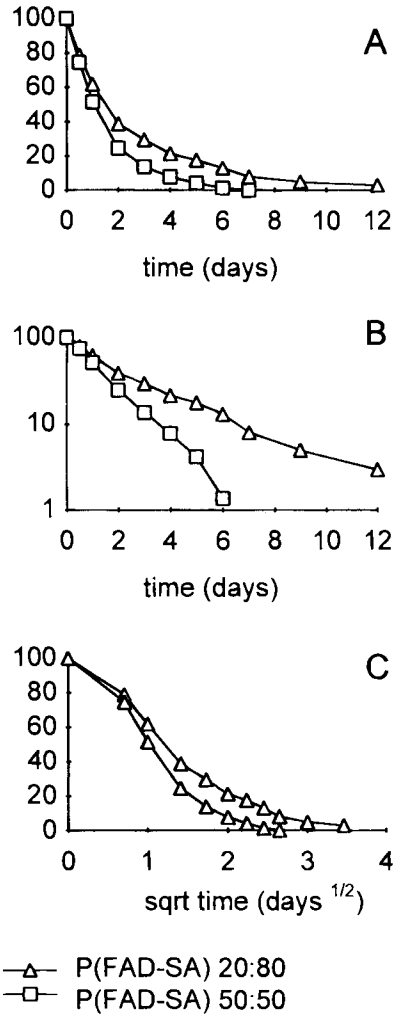

Fig. 7. *In vitro* release kinetics of PCA from P(FAD-SA) polymers. A: percentage remaining in the tablets vs. time; B: percentage remaining in the tablets on logarithmic scale vs. time; C: percentage remaining in the tablets vs. square root time.

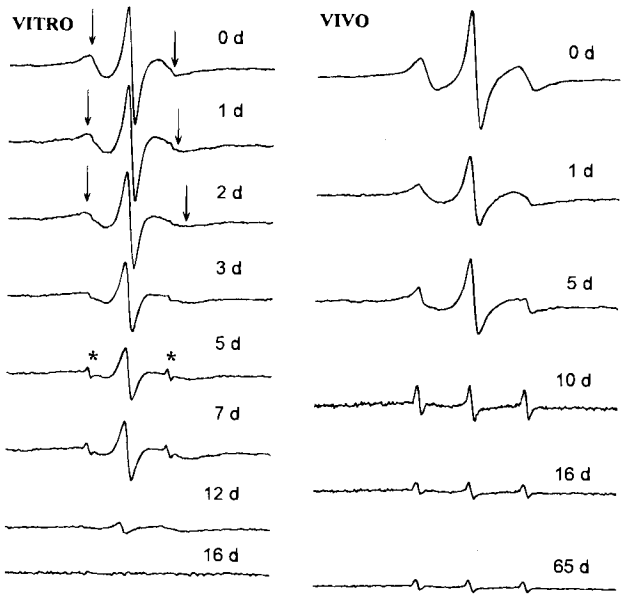

Fig. 8. 1.1 GHz EPR spectra of PCA loaded P(FAD-SA) 20:80 tablets: recorded *in vitro* after different times of exposure 0.1 M phosphate buffer (left); recorded *in vivo* after subcutaneous implantation in rats (right).

soluble monomers may potentially occur. This has been experimentally proved by Göpferich and Langer for P(CPP-SA) 20:80 polymers (20) and assumed also to occur for P(FAD-SA) polyanhydrides (19). The observed decrease of PCA mobility inside the polymer gives direct experimental evidence that SA crystallization induced coprecipitation of incorporated compounds does occur *in vitro* and *in vivo*. This process has a direct impact on the release kinetics.

The water penetration induced decreased nitroxide mobility (observation 1) is followed by the appearance of additional signals, which arise from water solubilized, highly mobile nitroxide molecules (observation 2). The detection of water solubilized PCA gives direct evidence that release of hydrophilic compounds of low molecular weight from P(FAD-SA) polymers, at least at later stages, is diffusion controlled. In contrast to P(FAD-SA), drug release from P(CPP-SA) 20:80 is not diffusion controlled, because only a decrease in signal intensity, but no change of the spectral shape has been detected (8). The difference in the release mechanisms can be attributed to the different characteristics of the polymer erosion layer: a rigid, porous solid for P(CPP-SA) 20:80; a flexible, gel-like layer for P(FAD-SA). The contribution of water solubilized PCA to the overall EPR signal intensity increases with time. Almost all PCA molecules are water solubilized *in vivo* after 10 days P(FAD-SA) 20:80) (Fig 8) and 8 days P(FAD-SA) 50:50.

The release of the nitroxide was slower *in vivo* compared to *in vitro* both for P(FAD-SA) 20:80 (Fig. 8) and P(FAD-SA) 50:50. The experimental results indicate that encapsulation contributes to the *in vitro/in vivo* discrepancy of release rates. The different *in vivo* release of PCA from P(FAD-SA) 20:80 (incomplete release after 65 days) and P(FAD-SA) 50:50 (complete release after 16 days) corresponds well to the different polymer clearance observed by MRI. Although completely water solubilized, PCA molecules are not released after day 16 from P(FAD-SA) 20:80 due to the encapsulation of the implant.

In summary, two noninvasive methods, Electron Paramagnetic Resonance Spectroscopy and Magnetic Resonance Imaging were combined for the first time to characterize the processes of drug delivery and polymer erosion from P(FAD-SA) polyanhydrides *in vitro* and *in vivo*. PCA was chosen as a model for hydrophilic drugs of low molecular weight. The results obtained by EPR spectroscopy let us conclude that drug release from P(FAD-SA) polyanhydrides is a complex event which includes water penetration induced monomer formation, crystallization of the monomer with decreased mobility of incorporated compounds inside the release matrix, drug solubilization and drug diffusion. MRI provides information concerning implant shape and size, edema, encapsulation and water content.

ACKNOWLEDGMENTS

K. Mäder gratefully acknowledges his support from Deutscher Akademischer Austauschdienst (DAAD) and Deutsche Forschungsgemeinschaft (DFG grant MA1648). A. Domb is affiliated with the David Bloom center of pharmacy

and the Grass center for drug design. This research used the facilities of the EPR and NMR Center at Dartmouth and was supported by NIH grant RR 01811 and NCDDG grant CA52857.

REFERENCES

1. A. J. Domb, S. Amselem and M. Maniar In: *Polymeric biomaterials,* Dumitriu S., Ed. Marcel Dekker, NY, 1994, pp. 399–433.
2. A. J. Domb, Ed., *Polymeric Site-specific Pharmacotherapy,* Wiley and Sons, Chichester, 1994.
3. R. Botwell, J. C. Sharp, A. Peters, P. Mansfield, A. R. Rajabi-Siahboomi, M. C. Davies, and C. D. Mella. *Magn. Res. Imag.* **12**:361–364 (1992).
4. G. Köller, E. Köller, W. Kuhn, and F. Moll. *Pharm. Ind.* **53**:955–958 (1991).
5. H. Brem, R. J. Tamargo, A. Olivi, M. Pinn, J. D. Weingart, M. Wharam, and J. I. Epstein. *J. Neurosurg.* **80**:283–290 (1994).
6. B. Reisfield, S. Blackband, V. Calhoun, S. Grossman, S. Eller, and K. Leong. *Magn. Res. Imag.* **11**:247–252 (1993).
7. R. Weissleder, K. Poss, R. Wilkenson, C. Zhou, and A. Bogdanov. *Antimicriobial Agents and Chemotherapy* **39**:839–845 (1995).
8. K. Mäder, G. Bacic, A. Domb, O. Elmalak, R. Langer, and H. M. Swartz. *J. Pharm. Sci.* **86**:126–134, (1997).
9. K. Mäder, H. M. Swartz, R. Stösser, and H.-H. Borchert. *Pharmazie* **49**:97–101 (1994).
10. G. R. Eaton, S. S. Eaton and K. Ohno, (Eds). *EPR Imaging and in vivo EPR.* CRC press, Boca Raton, 1991.
11. H. M. Swartz, G. Bacic, K. J. Liu, B. Gallez, K. Mäder, T. Shima, T. Nakashima, J. Jiang, J. O'Hara, T. Walczak. In: H. Ohya-Nishiguchi and L. Packer, (Eds.): Bioradicals detected by ESR Spectroscopy. Birkhäuser Verlag (1995), Basel, pp. 285–299.
12. K. Mäder, G. Bacic, and H. M. Swartz. *J. Invest. Dermatol.* **104**:514–517 (1995).
13. R. Stösser, K. Mäder, H. H. Borchert, W. Herrmann, G. Schneider, and A. Liero. In: H. Ohya-Nishiguchi and L. Packer, (Eds.): Bioradicals detected by ESR Spectroscopy. Birkhäuser Verlag (1995), Basel, pp. 301–320.
14. T. Yamaguchi, S. Itai, H. Hayashi, S. Soda, A. Hamada, and H. Utsumi. *Pharm. Res.* **13**:729–733 (1996).
15. K. Mäder, B. Gallez, K. J. Liu, and H. M. Swartz. *Biomaterials* **17**:459–463 (1996).
16. B. Gallez, V. Lacour, R. Demeure, R. Debuyst, F. Defehet, J. L. Keyser, and P. Dumont. *Magn. Res. Imag.* **12**:61–69 (1994).
17. A. J. Domb and M. Maniar. *J. Poly. Sci.:A Polym. Chem.* **31**:1275–1285 (1993).
18. L. Shieh, J. Tamada, Y. Tabata, A. Domb, and R. Langer. *J. Contr. Rel.* **29**:73–82 (1994).
19. L. Shieh, J. Tamada, I. Chen, J. Pang, A. Domb, and R. Langer. *J. Biomed. Mat. Res.* **28**:1465–1475 (1994).
20. A. Göpferich and R. Langer. *J. Poly. Sci.: A Polym Chem.* **31**:2445–2458 (1993).
21. M. P. Wu, J. A. Tamada, H. Brem, and R. Langer. *J. Biomed. Mat. Res.* **28**:387–395 (1994).